Korean J. Chem. Eng., **24**(1), 83-92 (2007)

Combustion characteristics of vacuum residue in a test furnace and its utilization for utility boiler

Ho Yong Park† **and Young Ju Kim**

Power Generation Laboratory, Korea Electric Power Research Institute,
103-16 Munji-dong, Yusung-gu, Daejeon 305-380, Korea
(*Received 12 March 2006 • accepted 14 September 2006*)

Abstract–Recently, increased attention has been exerted on the utilization of cheaper hydrocarbons fuel such as Vacuum Residue (VR). As a fundamental investigation for VR utilization, VR combustion tests were carried out in a test furnace with a fuel feed rate of 20 kg/h. As compared with heavy oil, VR used in this work is much more viscous and contains high percentages of sulfur, carbon residue and heavy metals. Successful fuel transportation and atomization has been achieved with the indirect heating of fuel by a thermia oil. The measured distributions of temperature, major species concentrations and solid samples along with the furnace revealed that the main reaction zone remains within about 1 m from the burner tip and the characteristics of VR flame are dependent on the ratio of fuel/air feeding rate. VR carbonaceous particles collected along with the furnace showed that their complete conversion would be a very essential factor for the utilization of VR as a fuel. Several issues for applying it to utility boilers have been investigated in line with the present results, and some suggestions have been made.

Key words: Vacuum Residue, Carbon Residue, Atomization, Viscosity

INTRODUCTION

Vacuum Residue (VR) is defined as the fraction of petroleum that does not evaporate under vacuum in the distillation process. It has an atmospheric equivalent boiling point over 525 °C and is produced as the bottom product from the vacuum distillation column in a refinery. Many conventional crude oils typically contain 10-30% residue. VR has often been used to manufacture asphalts around the world [Gray, 1994].

Much attention has been given to utilization of VR as a fuel for an Integrated Gasification Combined Cycle (IGCC) power generation system [Simbeck and Johnson, 2001; Choi et al., 2006]. Worldwide, several IGCC plants using VR have been in operation, while the market potential for residue-based IGCC is anticipated to be 120 GW by 2010 [Wolff et al., 2001]. Recently, Japan's first VR gasification combined cycle power plant with gross plant power output of 431 MW went into commercial operation in June, 2003 at the Negishi refinery [Sonoda et al., 2004]. Vigorous trial efforts have been made in Japan for application of VR as a fuel for conventional boilers as well. MHI (Mitsubishi Heavy Industries) provided 25 boilers fired by asphalt or high-viscosity heavy oils and a 475 ton/hr steam based boiler fired by VR, which began commercial operation in July 1998 [Hashimoto et al., 1998; Fujimura et al., 1999]. More recently, the operation results of a Vacuum Residue boiler in a 274 MW power generation plant were reported by Aoki et al. [2004].

As compared with the heavy oil, VR has many difficulties to be utilized in a utility boiler due to its extreme viscosity and high percentages of sulfur, nitrogen, carbon residue and heavy metals [Park and Seo, 2006]. It requires a more clean and stable combustion handling system than is conventionally available. The problems of VR in a commercial boiler include high temperature corrosion as well as SO_3 induced low-temperature corrosion, and emission of SO_x, NO_x and soot. The fuel handling system for fuel storage and transfer and cleaning of the fuel feed line after boiler shut-down would also require careful consideration for successful operation.

Features of VR as a combustion fuel are addressed by Ichinose et al. [1998], who performed combustion tests in a pilot scale, cylindrical test furnace. It was found that both NO_x and unburned carbon emissions in exhaust gas were at a comparable level with those in bituminous coal combustion. The NO_x emission in exhaust gas increased with increase of excess oxygen or decrease of OFA (Overfire Air). However, operation with high excess air in a utility boiler could cause severe low-temperature corrosion as well as decline in the boiler efficiency due to the higher sulfur content in VR than in other fuels. Although low excess air operation may be an effective method to reduce low temperature corrosion, it generally leads to increase in soot and unburned carbon emission in exhaust gas. Much research and development work may be required on the operation and environmental aspects as well as the fuel characteristics for application of VR in a utility boiler. The primary focus of this work is on the basic characterization of VR combustion in a test furnace in terms of gas temperature and major gaseous species at different fuel-air ratios. The characteristics of solid particles collected along with the furnace were also studied. With the present experimental results and literature survey, several aspects for VR utilization have been investigated.

EXPERIMENTAL

1. Fuel Analysis

The physical and chemical characteristics of VR used in the present work are given in Table 1, together with those of typical #6 heavy

†To whom correspondence should be addressed.
E-mail: hypark@kepri.re.kr

oil used in a utility boiler. The VR sample, supplied by Hyundai Oil Bank refinery in South Korea, gives similar properties as reported in the literature [Gray, 1994; Ichinose et al., 1998; Aoki et al., 2004]. The values for #6 heavy oil in Table 1 were mainly quoted from Basu et al. [2000], and other literature [Lefebre, 1989; Urban et al., 1992; Ichinose et al., 1998; Aoki et al., 2004]. Compared to #6 heavy oil, higher viscosity and percentages of sulfur, nitrogen, resident carbon and heavy metals are presented in VR. There are little differences heating value and density.

Table 1. Properties of VR and #6 heavy oil

Properties	Vacuum Residue	#6 Heavy oil
C (wt.%)	85.304	86.5-90.2
H (wt.%)	10.339	9.5-12.0
N (wt.%)	0.4520	0.2
S (wt.%)	3.7740	0.7-3.5
O (diff., wt.%))	0.1310	
CCR (wt.%)	20.765 (28-38)[1]	5-20[3]
Density (g/cm^3)	1.037	1.002-0.922
Heating value (kcal/kg)	10,100	9,648-10,523
Ni (ppm)	120	20-80[1,4]
V (ppm)	210	10-60[1,4]
Na (ppm)	110	30[1]
Asphaltene (wt.%)	13.1 (6-38)[2]	1-18[3]
viscosity in Cs at 38°C		260-750
at 93°C		40[5]
at 100°C	2,100	
at 120°C	600	
at 127°C		17[5]
at 140°C	225	

Cs=centistokes, [1]: Ichinose et al. [1998], [2]: Gray [1994], [3]: Urban et al. [1992], [4]: Aoki et al. [2004], [5]: Lefebre [1989].

2. Test Facility

The facilities for VR combustion tests consist mainly of a furnace, preheating system, exhaust gas treatment system, fuel and steam feeding system, and combustion air supply system. A schematic diagram of the present facilities is given in Fig. 1. The furnace was cylindrical, down-fired and operated at atmospheric pressure. Originally designed and constructed for the study of heavy liquid fuel gasification at high pressure, the furnace wall is refractory and has thermal insulation to minimize the heat loss. The radial thickness of the refractory and insulation is 200 and 147 mm, respectively, and the shell of the furnace is a 2 mm thick stainless steel tube. The inner diameter and height of the furnace are 200 mm and 3,200 mm, respectively. Each of the five temperature measuring ports is constructed together with a heat flux measuring probe. Opposite the temperature measuring ports, five sampling ports are also mounted for the measurement of gas concentration and particle collection.

The VR burner is installed on the top of the furnace, so that the flame develops along the furnace axis. The burner gun (105 mm in inside diameter) used throughout the experiment is operated with a removable internal-mixing steam-assist atomizer. The cap of atomizer houses an internal mixing chamber. The atomizing steam and VR are piped separately to the nozzle and mixed just before they

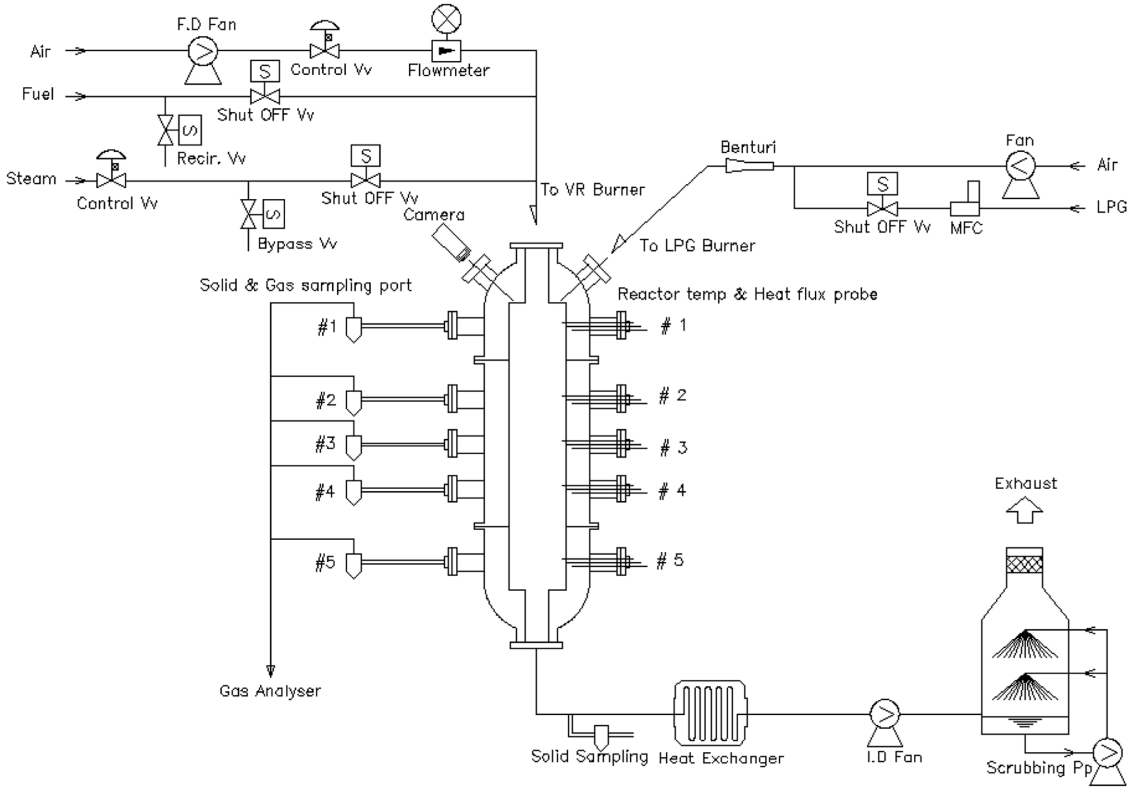

Fig. 1. Schematic diagram of combustion test facility.

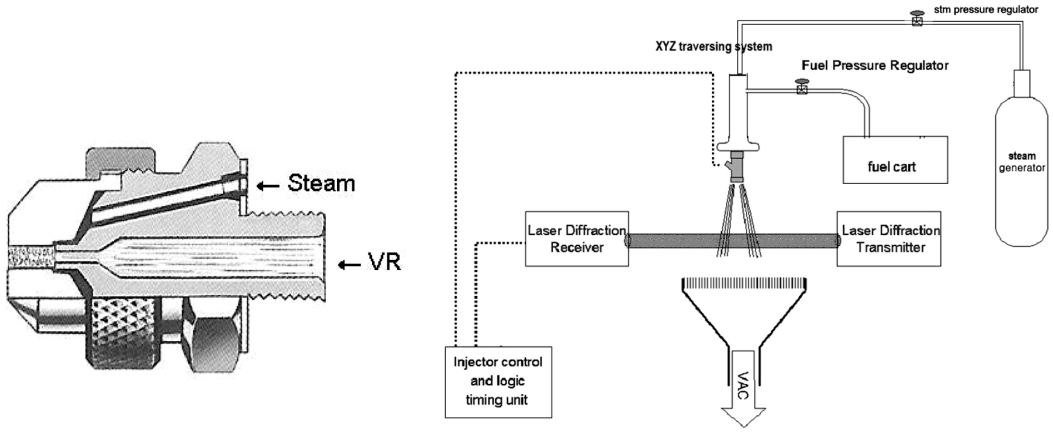

(a) Nozzle assembly (b) Atomizer test facility

Fig. 2. (a) Nozzle assembly, (b) Atomizer test facility.

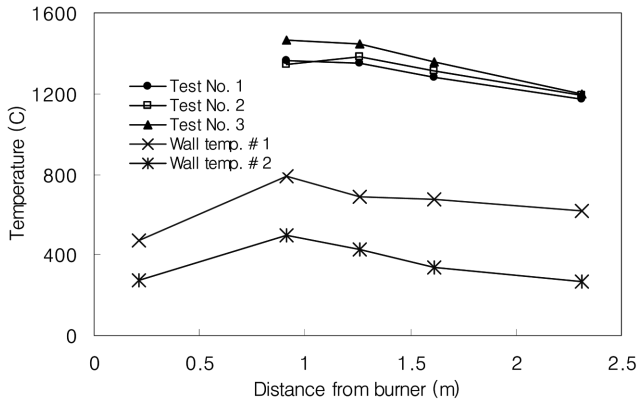

Fig. 3. Gas temperatures along the furnace axis and wall temperatures at test No. 2.

enter the atomizing slot of 2.5 mm in diameter. The spray characterization was made with Laser Light Scattering technique (HELOS system, Sympatec Gmbh) over a wide range of oil and steam flow rates. It included the Sauter Mean Diameter (SMD) at seven axial positions, their distribution, and the spray angles. A detailed diagram of the atomizer and a schematic diagram of atomizer test facility are given in Fig. 3(a) and (b), respectively.

A premixed LP gas burner was used to preheat the furnace and ignite the atomized VR-air mixture. Both LP gas and combustion air are separately supplied to a venturi type mixer, and the premixed LP gas-air mixture forms a flame with the low-pressure LP gas burner, which was installed at the top of the furnace, biased from the furnace axis (See Fig. 1).

The downstream end of the furnace is connected to the exhaust gas treatment system. Following combustion in the furnace, the products are exhausted along the water-cooled stainless steel duct into the atmosphere by a variable speed centrifugal exhauster (I.D fan in Fig. 1). Here, the furnace pressure is maintained at a negative pressure of about 20 mm H_2O. A heat exchanger is installed between the exhauster and the furnace outlet in order to cool down the flue gas temperature. After passing the exhauster, the flue gas goes to a scrubber having a wire-wool filter, and is emitted to the atmosphere.

As seen in Table 1, the viscosity of VR is very high so that VR temperature is increased up to about 140 °C in order to transfer it to the burner nozzle. To increase VR temperature, an indirect heating method by using a thermia oil B (Shell) was adopted in this work. Thermia oil B, heated to over 230 °C in an oil heater, was circulated inside the storage tank through a spirally constructed stainless zthe storage tank. When VR temperature in the tank reaches about 140 °C, the gear pump starts to feed VR to the burner. All feed lines are constructed of two concentric stainless steel pipes, passing VR along the inner pipe and thermia oil in the annulus. The flexible feeding line from the outlet of feeding system to the burner was wrapped with the electrical heating element in order to increase VR temperature over 170 °C to meet the sufficient atomization. The gear pump was sustainable at a maximum fluid temperature of 250 °C and pressure of 20 bar. The VR feeding rate was controlled by the gear pump speed.

A 12 kW electrical boiler, which is capable of producing a steam flow rate of 12 kg/hr at 15 bar, was used to generate atomizing steam. The pressure and temperature of steam for the present atomization were about 1 bar and 170 °C, respectively. A 7.5 kW centrifugal blower supplied the combustion air to the burner. Pneumatic control valves, which are installed before the burner, were used to control both the flow rates of steam and combustion air.

3. Test Procedure and Condition

Preheating of the furnace is necessary to ignite atomized the VR particles and stabilize the flame by means of radiative feedback from the hot wall. Preheating by the LP gas burner took about 6 hours. When the furnace wall temperature, indicated by the thermocouple located in 50 mm from the inside wall and at axial position of 910 mm (at port No. 2) from the burner, reaches about 600 °C, VR is supplied to the burner with atomizing steam and combustion air. The LP gas-air preheat flame was extinguished after confirming a stable VR-air flame, and then the experimental conditions were adjusted.

The time-averaged gas temperature within the furnace was measured with a radially traversing 0.125 mm B-type thermocouple at five axial locations along the furnace. The measurements of radial

gas temperature were made at six points from the inner furnace wall to the center of the furnace. At the first port (x=210 mm), the radial gas temperature measurement was only available at 10 mm from the inner wall since the fast injection of atomized VR particle caused failure of the ceramic-shielded thermocouple. The five heat flux probes, made of two K-type thermocouples with a distance of 100 mm, were installed at the same locations as the gas temperature measurements.

A water-cooled probe, comprising two concentric stainless steel tubes (4 mm i.d and 8.2 mm o.d) and the annulus between them forming a water jacket, was used to extract gas and solid samples from the furnace. To separate the particles from the sampled mixture, a trap was used. The sampled gas was condensed with a gas conditioning system (M5210, Baldwin Ltd.), and the metered gas was passed through a filter and dryer to the gas analyzer (IMR 3000, Environmental Equipment Inc.) for O_2, CO, CO_2, NO and SO_2 measurements. Iso-kinetic sampling [Chigier, 1991] was not made in this work because of the complexities in the velocity field itself and the sampling direction perpendicular to the combusted gas flow. Considering a simple volumetric balance between the sampling flow rate and the control volume of combusted mixture, a spatial resolution caused by the non-isokinetic sampling was calculated. The present gas sample was collected in the control volume of about 10 mm diameter from the sampling probe tip.

The experimental conditions are summarized in Table 2. For VR combustion and atomization test, the VR feed rates varied at 10.90, 12.01 and 14.21 kg/hr, while the combustion air was kept constant as a 97.5 m^3/hr. From the ultimate analysis given in Table 1, the equivalence ratio, ϕ, for test No. 1, 2 and 3, was calculated to be 1.169, 1.288 and 1.525, respectively [Singer, 1991]. A steam flow rate of 4.68 kg/hr was commonly used for each combustion test. Atomizer tests depending on the steam feed rate were also carried out, and their conditions are given, in Table 2, as test No. 4, 5 and 6.

RESULTS AND DISCUSSION

1. Characteristics of VR Atomization

As seen in Table 1, the viscosity of VR is extremely high, compared with heavy oil. In the present work, the temperature of VR should be increased up to 140 °C for proper transportation to the burner and further increased over 170 °C for proper atomization. These were achieved with the indirect heating by using thermia oil in the fuel feeding system and electrical heating of flexible fuel feed line, as mentioned above. After ascertaining the excellent VR supply to the burner nozzle, we carried out an atomization test over a wide range of fuel and steam feed rates. For experimental conditions in Table 2, Volume mean diameter (VMD), sauter mean diameter (SMD) and mean diameter (MMD) of atomized VR particles were measured by using the Helos system (Sympatec Gmbh). The measured values in SMD, VMD and MMD at a distance of 170 mm from the nozzle are summarized in Table 3. The spray angles for test conditions turned out to be about 20°, commonly. For test Nos. 1, 2 and 3, SMD varied from 68.4 to 84.9 mm as the fuel feed rate increased from 10.90 kg/hr to 14.21 kg/hr with the constant steam flow rate. The same tendency was observed with VMD and MMD. The effects of steam feed rate on the droplet size were also studied at the conditions given in Table 3. The steam feed rates used for this test were 3.64, 4.68 and 5.68 kg/hr while the VR feed was fixed at a rate of 12.01 kg/hr. It was found that the minimum droplet size occurred at a steam feed rate of 4.685 kg/hr. Generally, the increase of atomizing steam results in a decrease in atomized droplet size due to the increased energy input. However, for the present nozzle, further a increase in steam feed rate over 4.685 kg/hr does not much affect the droplet size. For the VR combustion test, the atomizing steam was fed to the nozzle at a constant rate of 4.68 kg/hr.

Table 3. The measured droplet size at x=170 mm with increase in fuel and steam feed rate

Test no.	Sauter mean diameter (μm)	Volume mean diameter (μm)	Median diameter (μm)
1	68.4	146.3	122.5
2	71.3	147.5	124.6
3	84.9	188.1	158.6
4	72.5	174.8	145.7
5 (=2)	71.3	147.5	124.6
6	77.0	174.3	147.3

2. Axial Gas and Wall Temperatures

Fig. 3 shows the gas temperature profiles at the center of the furnace for the test Nos. 1, 2 and 3. As seen in Table 2, each test condition represents a different equivalence ratio with the same amount of atomizing steam flow. The profiles of wall temperature at Test No. 2, indicated by K type thermocouples radially embedded at 50 and 100 mm from the inner wall, are also given in the same figure.

For test Nos. 1, 2 and 3, the measured peak gas temperatures at furnace axis are 1,365, 1,385 and 1,464 °C, respectively. This coincides with the results of Gollahalli et al. [1984], who carried out #6 heavy oil combustion tests in a test furnace, that is, the increase of fuel flow rate increases the peak values in axial temperature. It is not surprising since the increase in fuel feed rate indicates an increase in energy input, resulting in a higher peak temperature. For

Table 2. Experimental conditions

Test no.	Fuel feeding rate (kg/hr)	Air feeding rate (Nm^3/hr)	Steam feeding rate (kg/hr)	Equivalence ratio (ϕ)	
1	10.90	97.5	4.685	1.169	Combustion/Atomization
2	12.01	97.5	4.685	1.288	Combustion/Atomization
3	14.21	97.5	4.685	1.525	Combustion/Atomization
4	12.01	97.5	3.640	1.288	Atomization
5 (=2)	12.01	97.5	4.685	1.288	Atomization
6	12.01	97.5	5.680	1.288	Atomization

the three tests, the gas temperature peaks near 1 m from the burner tip, and further downstream, slowly decreases. As already discussed, the gas temperature at port No. 1 (x=210 mm) was not measured. However, it is easily anticipated that the initial gas temperature rise up to the peak temperature would be steeper than the temperature decline downstream. Both the radiative heat loss as well as the heat loss across the furnace wall could explain the observed decrease of gas temperature downstream. The conductive heat transfer through the wall can be calculated from the measured wall temperatures given in Fig. 3.

The wall temperature profile for only the second test was given in Fig. 3 since other tests gave a similar profile. The highest wall temperature would be an index in identifying the flame position, as suggested by Villasenor and Escalera [1998] in their heavy fuel oil combustion test in a 500 MW test furnace. Here, it should be noticed that the present wall temperature profile might result from the long preheating. A similar wall temperature profile was already identified during the LP gas preheating. Therefore, it is difficult to assert the position of VR-air flame from the gas and wall temperature profiles and worth while to check on the profiles of major species concentration in the furnace.

In the present work, a thorough flame observation along with the furnace was not possible since the camera for flame observation was only installed at the top of the furnace (See Fig. 1). However, the color photographs observed with this camera showed that the steam-atomized VR flames were yellow and very luminous.

3. Radial Gas Temperatures

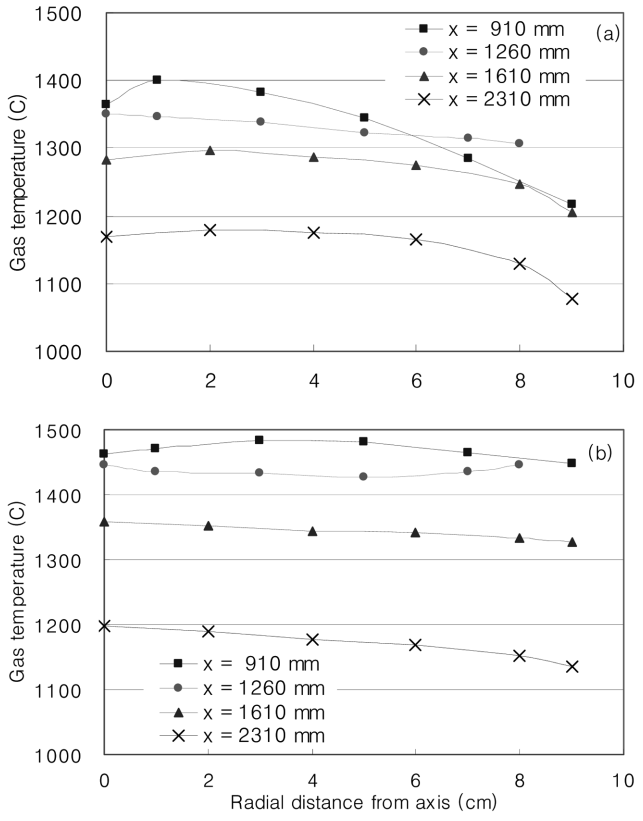

Fig. 4. Radial temperature measurements: (a) Test No. 1, (b) Test No. 3.

Fig. 4(a) and (b) show the radial gas temperature distributions for test Nos. 1 and 3 at ports 2, 3, 4 and 5, which correspond to 910, 1,260, 1,610 and 2,310 mm from the burner tip. For all tests, it can be seen that the measured radial gas temperatures increase with increases in fuel feed rate. The maximum gas temperatures for tests 1, 2 and 3 occurred typically at an axial position of 910 mm, and they were 1,400, 1,433 and 1,483 °C, respectively. It is noted that, at x=910 mm, the gas temperature starts to increase from the furnace center, reaches the peak temperature and gradually decreases to the inner furnace wall. This is also identified with the combustion of #6 heavy oil in a test furnace [Gollahalli et al., 1984], especially near the nozzle. In the present work, the crest of the radial gas temperature profile moves to the inner wall with an increase in the fuel feed rate. With respect to tests. 1, 2 and 3, the peak temperatures occur at the radial direction of 10 mm, 30 mm 40 mm from the furnace axis. The shift of the peak temperature to the wall with increasing fuel feed rate might be attributed to the alteration of the radial distribution of atomized VR particles or the flow field such as a recirculation zone. At an axial position of 1,260 mm, the temperature profile becomes even, and further downstream the radial gas temperature distributions appear to be thermally fully developed.

In Test No. 3, the overall shapes of radial temperature distribution are somewhat different from those in test No. 1, giving a little variation in the radial direction. It might be explained as follows. The increased fuel feed rate produce more volatiles and carbon particles. In this condition, there is a possibility that the combustible volatiles and carbon char are uniformly dispersed at a relatively small cross sectional area of the furnace, and the evenly distributed combustible mixtures may result in a little change in a radial temperature distribution. In reality, large amounts of unburned carbon particles were collected at exhaust gas in Test No. 3 while carbon particles in Test Nos. 1 and 2 were rarely collected.

4. Gaseous Species Concentrations

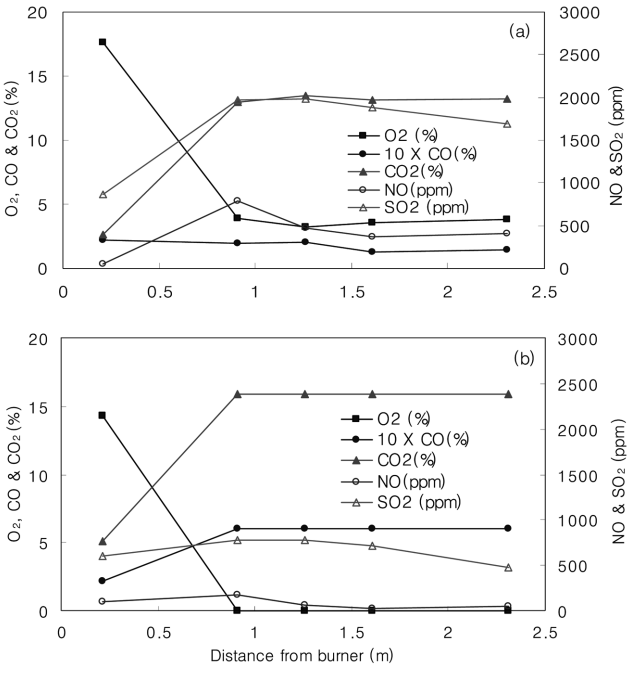

Fig. 5. Concentration measurements: (a) Test No. 1, (b) Test No. 3.

Fig. 5(a) and (b) present the axial concentration profiles of O_2, CO, CO_2, NO and SO_2 for test No. 1 and 3, measured at 20 mm (r=80 mm) from the furnace inner wall. All measured values are moisture free. Fig. 5(a) and (b) show the oxygen decreases rapidly from the burner, and then the profile is flattened after an axial distance of 910 mm, while CO_2 and CO are formed rapidly in the first 910 mm of the furnace and then reaches values close to the exhaust emission level. In most flames, the axial concentration of CO reaches a peak value in the near burner region and the location of its maximum value precedes the occurrence of the peak value in CO_2 concentration. These trends were found in the observations of Gollahalli et al. [1984] and Park and Seo [2006], although the magnitudes are different. In the present study, it was not possible to get concentrations of CO and CO_2 in the first 910 mm from the burner. However, considering O_2 and CO_2 profiles together with the axial temperature profiles given in Fig. 2, the main reaction zone seems to be formed within 910 mm from the burner tip. The leanest flame, Fig. 5(a), gives about 5% O_2 downstream, while the complete depletion of O_2 downstream is found in the richest flame, Fig. 5(b). The concentrations of CO for the three tests reflect the equivalence ratio of each VR-air flame; that is, CO concentration is relatively low at fuel-leanest flame, and high at fuel-richest flame. The gas analyzer used in the present work, IMR 3000 (Environmental Equipment Inc.), has a limit in measuring CO and CO_2 concentrations. Concentration measurements over 6,000 ppm for CO and 15.9% for CO_2 are not possible. In fact, concentrations of CO and CO_2 measured downstream in Fig. 5(b) exceeded these ranges, so that only the upper limit values are presented. The actual values will be higher than the measured ones.

The NO concentration in Fig. 5(a) and (b) shows NO increases mainly in the reaction zone and reaches a peak value at x=910, then the profiles are flattened downstream. Downstream NO concentration of Test No. 1 is similar to that of Test No. 2, and the minimum emission of NO is attained in the fuel-richest flame (Test No. 3). Lower value of NO emission at fuel rich condition has been reported elsewhere [Miller and Bowman, 1989; Pfefferle and Churchill, 1986; Moleo, 1998]. In the reducing atmosphere of fuel-rich conditions, the formation of N_2 would be favored with respect to that of NO. Also, the formation of fuel-NO has a great dependence on the oxygen concentration. As found in heavy oil combustion experiments by Moleo [1998], it is anticipated that the high yields of fuel-NO are attained in fuel-lean mixtures, on the while low yields are found in fuel-rich mixtures.

In the typical heavy oil combustion environment, SO_2 is the predominant sulfur compound with high conversion of fuel-S to SO_2 [Ichinose, 1998]. With the presence of oxygen as seen in Fig. 5(a), sulfur is likely to be oxidized to SO_2. The fuel richest condition, test No. 3, gives about a quarter of SO_2 emission in test No. 1 and 2. The presence of other sulfur species such as H_2S, S_2, SH and S, resulting from the oxygen shortage, is responsible for the decrease of SO_2 in fuel-rich combustion environments [Cullis and Mulcahy, 1972; Molero, 1998].

5. Characteristics of Particulates Collected Along the Furnace

The physical and chemical characterization of VR particles collected along the furnace includes particle size distribution, scanning electron microscopy (SEM), and EDX analysis and measurement of chemical composition. Due to the lack of collected sample, elemental analysis was not carried out for all solid samples. Here, it should be noticed that most samples were obtained at the period of test No. 3, which is the fuel-richest flame. Small amounts of particles were found at test Nos. 1 and 2. When the fuel feed rate is increased keeping air flow rate constant, the atomization becomes poor and heat abstraction by the fuel increases. Consequently, the coarser atomization delays evaporation and combustion of droplets, resulting in the higher portion of carbonaceous particles in test No. 3.

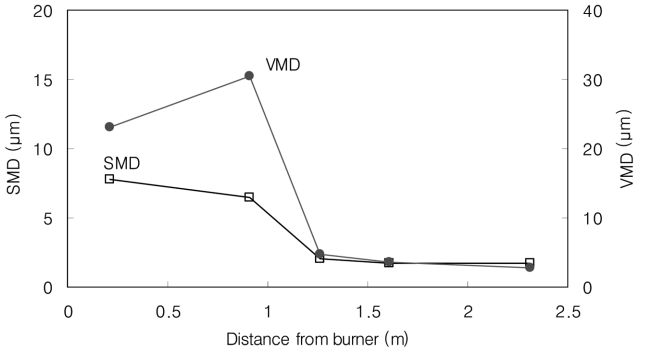

Fig. 6. Variations in particle size along with the furnace axis.

The changes in particle diameter and size distribution of VR carbon particles were determined by using a laser light scattering technique. The HELOS system supplied by Sympatec Gmbh was used for the measurements. The obtained volume mean diameters (VMD) and sauter mean diameter (SMD) at axial positions of 210, 910, 1,260, 1,610 and 2,310 mm are given in Fig. 6. The fact that the particulates collected at x=210 mm are smaller than those at x= 910 might be attributed to the recirculation of lighter atomized-VR particulates, while the bigger particles could exist in the main reaction region near x=910 mm. The particle distribution predicted from the preliminary simulation supports the re-circulation of the smaller particles near the burner. As seen in Fig. 6, the diameter decreases abruptly from the maximum value of 30.6 (x=910 mm) to 4.72 mm (x=1,260 mm), suggesting that the particle reaction mainly occurs before x=1,260 mm. A continuous, slight decrease in particle diameter is observed downstream.

The surface structure of solid samples was studied with a JEOL JSM 6360 scanning electron microscope (SEM). EDX analyses were also carried out with INCA X-sight (Oxford Instruments). SEM photographs of the particles collected at each sampling port are shown in Fig. 7. The photograph of the sample collected at port No 1, Fig. 7(a), reveals that the blow-holes range from about 1 to 9 μm in diameter and the smaller particles tend to be more sponge-like, having smaller blowholes. Some broken particles seem to be layered and flaky, and tiny and agglomerated particles appear on the surface of a large particle. The large particles are spheroidal and have many blow-holes which seem to be connected to the inner cellular structure. These are often called cenospheres. The formation mechanism and characteristics of cenospheres in heavy oil combustion have been reported elsewhere [Marrone et al., 1984; Clayton and Back, 1989; Northrop et al., 1991]. In most case disruptive ejection of volatile fuel components from the droplet and thermal decomposition of heavy fuel components inside the droplet have been accepted as an initial stage of the coke formation process. The volatiles that dif-

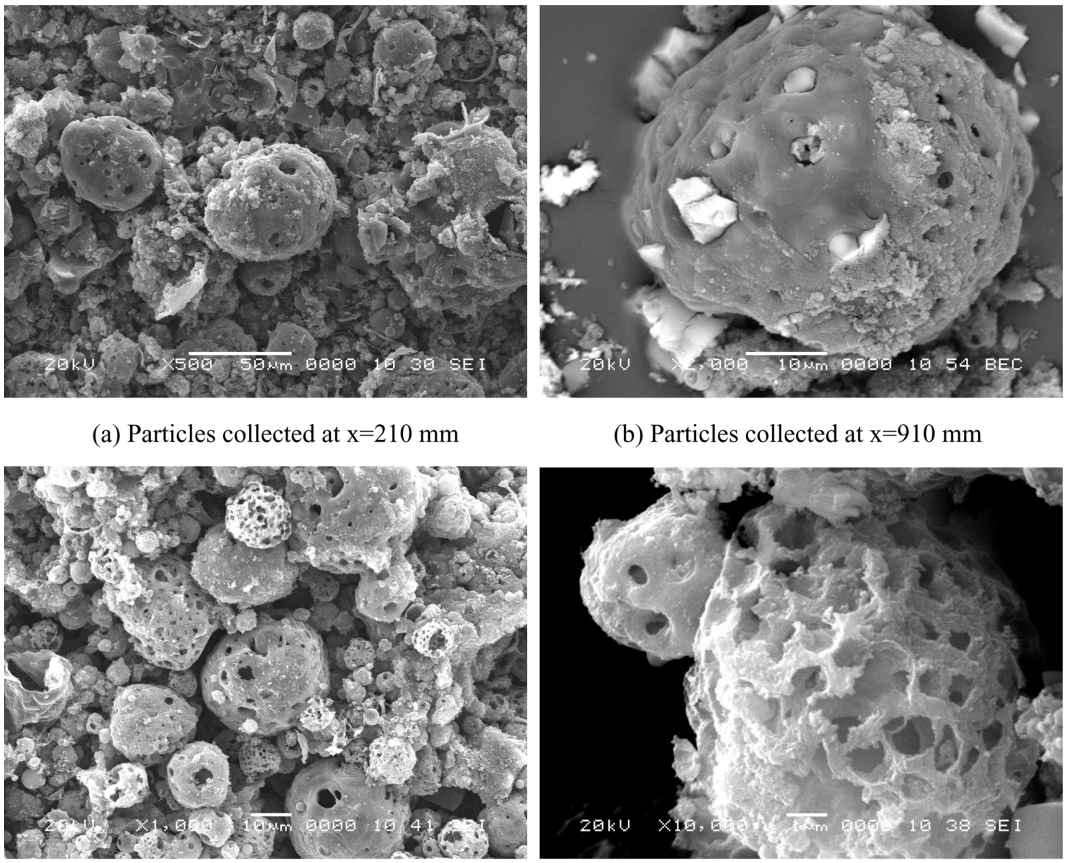

(a) Particles collected at x=210 mm (b) Particles collected at x=910 mm

(c) Particles collected at x=1260 mm (d) Particles collected at x=2310 mm

Fig. 7. SEM photographs of VR particles.

fuse to the surface evaporate and form a diffusion flame. This diffusion and evaporation of the volatiles cause a viscous shell to form consisting of the remaining asphaltene and resin. The shell then slows further diffusion of volatile component from the interior. As the interior temperature increases, additional volatile components vaporize, increasing the size of the drop with fuel escaping through a weak porting of the shell. Eventually, a hollow shell residue remains at the end of the vaporization [Clayton and Back, 1989; Moszkowicz et al., 1996]. The present cenospheres represent a similar shape and surface structure of those derived from heavy oil combustion [Clayton and Back, 1989; Hsieh and Tsai, 2003; Northrop et al., 1991].

The magnification of a large particle collected at port No. 2 is shown in Fig. 7(b). A smooth surface having many blow-holes can be seen. Very tiny particles on the particle surface are found and seem to be agglomerated soot particles. The co-existence of carbon char and soot particles was also identified in the VR combustion test performed by Ichinose et al. [1998]. Generally, soot is formed in gas-phase reactions of vaporized organic matter in a complex process involving fuel pyrolysis, polymerizations, nucleation, and particle growth [Richter and Howard, 2000; Linak et al., 2003]. In oil combustion, fuel droplets burning in envelope flames are subjected to very high temperatures, leading to fuel evaporation and thermal cracking of the large molecular structures, thus resulting in species of higher C/H ratio than the fuel source. Eventually, nucleation and growth take place, forming particles with C contents ranging from 90 to 98% [Molero, 2004]. Soot appears after 1 ms of combustion and may grow up to 1,000 μm in 10 ms and then agglomerate [Glassman, 1986]. In coal flames, soot is thought mainly to evolve directly the tar, which is a mixture of heavy-molecular-weight hydrocarbons and the most abundant species of volatile components. Tar undergoes secondary pyrolysis by cracking and polymerization, producing light gases and soot [Serio et al., 1987; Ma et al., 1996]. The process of soot formation in coal flames appears to be very fast and soot particles to form in the particle boundary layer flow around the particle and agglomerate in the particle wake [Seeker et al., 1980; Nenniger et al., 1983; Thimothy et al., 1986; Ma et al., 1996]. It has been known that soot is most likely to be formed in fuel-rich conditions. In this study, soot was mainly found near the burner zone and rarely found downstream, indicating that soot begins to form in the vicinity of the nozzle, starts to coagulate away from the nozzle, and is oxidized with oxidants (presumably O_2) along the furnace.

Particles collected at port No. 3 and 5 are shown in Fig. 7(c) and (d). The particles are more sponge-like and smaller spheroids than those collected at port No. 1 and 2. Some particles seem to be hollow and have voids within the shell. Crushed particles are found in places and agglomerated ones are also found. Fig. 7(c) and (d) suggest the particles become smaller and more sponge-like as the particle oxidation proceeds.

For a comparison of VR carbonaceous particles with particles

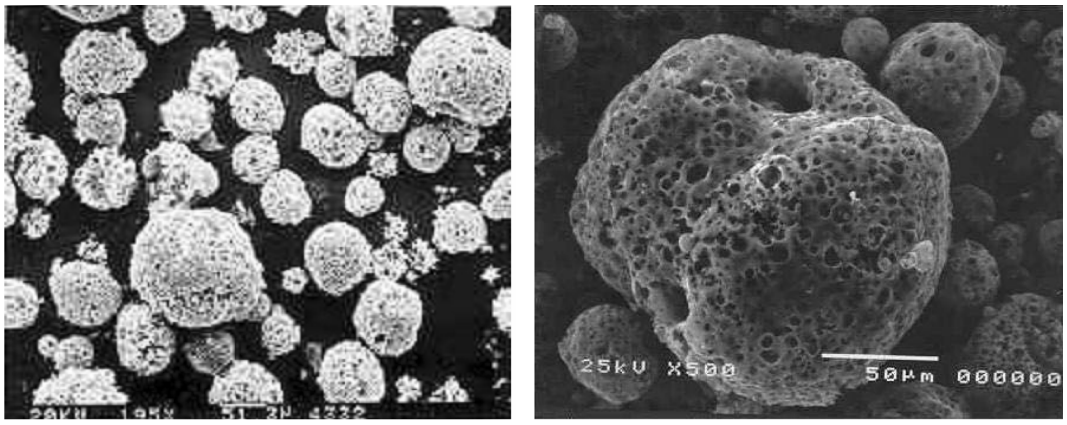

(a) Solid particles from heavy oil power plant (b) Magnification of solid particle

Fig. 8. SEM photographs of solid particles collected from heavy oil fired-power plant.

derived from heavy oil combustion, samples taken from the ash collector at a heavy oil-fired power plant were investigated, and photographs are given in Fig. 8(a) and (b). In contrast to VR particles, the particles appear to be more identical and spherical than those in VR combustion. Fig. 8(b) shows the more sponge-like, porous surface structure than that of VR carbonaceous particles.

EDX analysis taken for the typical particles shown in SEM photographs gave carbon values of about 72-84 wt% for carbon, 6-13 wt% for oxygen, 3-6 wt% for sulfur. Small amounts of heavy metals were also identified. For example, EDX analysis with respect to the particle located in the center of Fig. 7(c) gave values of 77.94% C, 10.77% O, 5.9% S, 0.3% V, 0.29% Cr, 1.9% Fe, 0.46 Ni, 1.56 Cu and 0.88 Zn % (weight basis).

Due to the lack of collected samples, elemental analysis was possible only for two samples taken from the sampling ports 1 and 5. The obtained values of C, H, N, S and unidentified materials for the sample collected at port No. 1 were 68, 17, 3.40, 1.29, 5.16 and 21.97 wt%, respectively. For the sample collected at port No. 5, the corresponding values were 43.54, 1.45, 1.55, 10.35 and 43.11 wt%. Oxygen was not included in the elemental analysis. It is difficult to make an acceptable interpretation with these values. However, the findings of nitrogen and sulfur in samples suggest that some of these elements are not fully devolatilized from the atomized VR particles and still remained in the solid particles, especially in fuel-rich condition.

6. VR Utilization as a Fuel for Utility Boiler

Compared with heavy oil, Vacuum Residue (VR) is extremely highly viscous and contains high percentages of nitrogen, sulfur, carbon residue and heavy metals. For its use as a fuel for a commercial boiler, several issues have been discussed elsewhere [Ichnose et al., 1998; Park and Kim, 2006]. As given in Table 1, the viscosity of VR used in this study is much greater than that of #6 heavy oil. In general, the heavy oil in the utility boiler increased to about 90 to 100 °C for proper atomization at two-fluid, steam or air-assisted burner. At these temperatures, the viscosity of heavy oil ranges approximately 20 to 30 cP, which is known as the ideal value for atomization [Ichinose et al., 1998]. Fig. 9 shows the plots of viscosities against the temperature for the present VR and #6 heavy oil in Table 1, together with VR obtained form SK refinery. Great

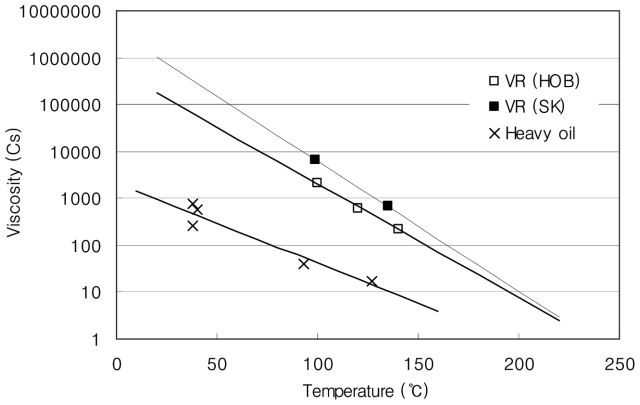

Fig. 9. Viscosities of VR and #6 heavy oil.

attention should be paid to the extremely high viscosity of VR. The present heating method with thermia oil might be adequate for the pilot scale test facility; however, its commercial application seems to be very difficult. In oil-fired utility boilers for power generation, the oil heater has been adopted to increase the heavy oil temperature to about 100 °C. An oil heater usually uses high pressure and temperature steam, which is extracted from the steam turbine; the capacity of oil heater should be increased for the use of VR as a fuel.

The resident carbon of the present VR is 20.765 wt%. In the literature it has been reported to vary from about 10 to 40 wt%, which is much higher than that of a typical heavy oil [Gray, 1994; Ichinose et al., 1998]. Generally, the greater the percentage of resident carbon found in fuel, the more unburned carbon can be found in the exhaust gas. In heavy oil combustion, it is convenient to introduce the coke formation index (CFI) which is defined as the mass fraction of the initial fuel droplet that is converted to coke [Urban et al., 1992]. CFI is related to fuel properties such as asphaltene content and carbon residue. It has been known that higher asphaltene content indicates a higher potential to produce particulate emissions, and carbon residue gives an indication of the coking tendency of a particular fuel. Also, it has been reported that less oxidation time was required for coke particles that were low in asphaltenes [Villasenor and Garcia, 1999]. Urban et al. [1992] reported values of CFI of over 40 dif-

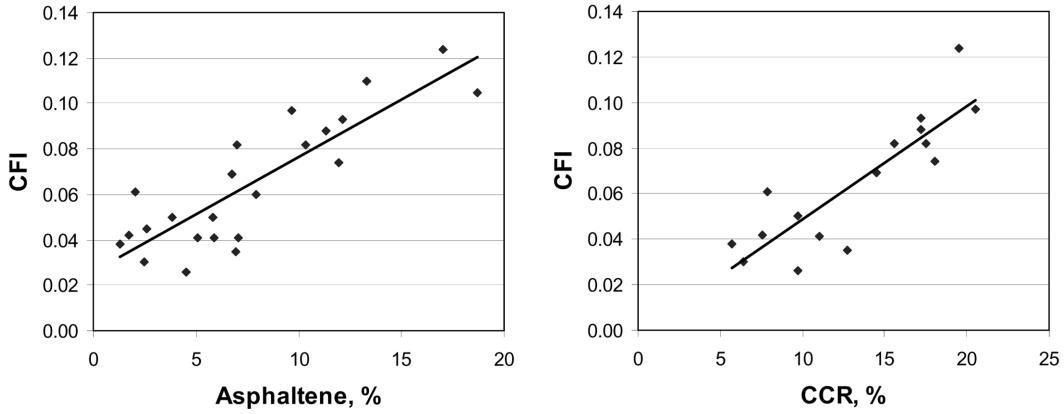

(a) CFI against asphaltene (%) (b) CFI against CCR(%)

Fig. 10. Relationship among CFI, asphaltene and CCR.

ferent residual fuels under typical boiler conditions. As seen in Fig. 10, their study showed that CFI increases with increasing fuel asphaltene content and Coradson Carbon Residue (CCR). When CFI is plotted against both properties, linear correlations are obtained as follows:

$$CFI=0.00507*(\text{Asphaltene }\%)+0.02588 \quad (1)$$

$$CFI=0.00496*(\text{CCR }\%)+0.00083 \quad (2)$$

For the VR properties in Table 1, CFI is calculated to be 0.0918 and 0.1022, based on asphaltene content and CCR, respectively. From Table 1, the values of CFI for #6 heavy oil would be somewhat lower than that for VR. In VR application to the boiler or furnace, a higher CFI value for VR than heavy oil indicates that greater residence times are required to oxidize VR carbonaceous particles if their droplet size is the same as those in heavy oil combustion.

The values of nitrogen, sulfur and heavy metals contained in VR are generally higher than those contained in heavy oil. High values in fuel nitrogen force one to adopt low NO_x technologies such as low NO_x burner, staged combustion and SCR (Selective Catalytic Reduction), to satisfy environmental regulations. From the experimental works of Ichinose et al. [1998], OFA (Over-Fire Air) has been proven as an example of excellent technique to reduce NO_x level at exhaust. Staged combustion as with OFA has advantages in reducing particulate emission as well as NO_x in exhaust [Villasenor and Garcia, 1999]. The emulsification of residual oil might be another method for the reduction of NOx and soot particles [Gollahalli et al., 1984].

The principal problems associated with boilers firing high-sulfur oils are high-temperature corrosion of superheater and reheater tubes by low-melting-ash deposits, and low temperature corrosion of air heater, ducts, and dust collector equipment by condensed sulfuric acid in the flue gas. It is also known that the extent of high temperature corrosion is accelerated by the presence of heavy metals such as V and Na in the molten slag on the tube [Park and Kim, 2006].

CONCLUSIONS

Regarding the use of VR as a fuel for utility boilers, a number of serious problems should be overcome, and several aspects of VR utilization have been pointed out with the results of the present work. In the present work, VR temperature had to be increased to over 140 °C and 170 °C for stable VR transfer and atomization, and these were accomplished by the indirect heating of VR by a thermia oil. From the distributions of axial gas temperature and species concentration, and collected particle size, the main reaction zone in all experimental conditions seemed to be with 1 m from the burner tip. As the fuel feed rate increases, the radial location of the peak gas temperature moves to the inner furnace wall, and it might be attributed to the alteration of flow field or to the different distribution of atomized VR particles. The VR carbon particles collected along the furnace show that the particles become smaller and more sponge-like as the particle oxidation proceeds, and the existence of agglomerated soot particles was found upstream, but rarely downstream. Several aspects for VR utilization have been investigated in relation to the high viscosity, poor reactivity of VR carbon char, NO_x, SO_x, particlulate emission, and low/high corrosion. The basic information for VR combustion, obtained through the present work, would be primarily valuable to researchers and engineers who are making efforts to apply VR as a fuel for a utility boiler.

RERERENCES

Aoki, H., Fukushima, H. and Yoshida, T., "Design and operation results of vacuum residue firing boiler," *The Thermal and Nuclear Power*, **55**, 1356 (2004).

Basu, P., Kefa, C. and Jestin, L., *Boilers and burners*, Springer, New York (2000).

Chigier, N., *Combustion measurements*, Hemisphere Publishing Corporation, New York (1991).

Choi, Y. C., Lee, J. G, Yoon, S. J. and Park, M. H., "Experimental and theoretical study on the characteristics of vacuum residue gasification in an entrained-flow gasifier," *Korean J. Chem. Eng.*, **23**, (2006).

Clayton, R. M. and Back, L. H., "Physical and chemical chracteristics of cenospheres from the combustion of heavy fuel oil," *Journal of Engineering for Gas Turbines and Power*, **111**, 679 (1989).

Cullis, C. F. and Mulcahy, M. F. R., "The kinetics of combustion of gaseous sulphur compounds," *Combustion and Flame*, **18**, 225 (1972).

Fujimura, K., Mastumoto, H., Arakawa, Y., Fujii, H. and Mizoguchi, T., "Development and operation results of VR firing boiler," *Mitsubishi Juco Giho*, **36** (1999). See also http://www. mhi.co.jp/tech/htm/9362/e936211a.htm.

Gollahalli, S. R., Nasrullah, M. K. and Bhashi, J. H., "Combustion and emission characteristics of burning sprays of a residual oil and its emulsions with water," *Combustion and Flame*, **55**, 93 (1984).

Gray, M. R., *Upgrading petroleum residues and heavy oils*, Marcel Dekker, Inc., New York (1994).

Glassman, I., *Combustion*, 2nd Ed., Academic Press, Orlando (1987).

Hashimoto, A., Ichinose, T., Fujimura, K., Kaneko, S., Hishida, M. and Arakawa, Y., "Development of low excess air combustion technology for residual oil fuels," *Mitsubishi Juco Giho*, **35** (1998). See also http://www. mhi.co.jp/tech/htm/8351/e835108a.htm.

Ichinose, T., Fujimura, K., Takeno, K., Motai, T., Arakawa, Y. and Fujii, H., "Combustion characteristics and pollution minimum technology for VR (Vacuum Residue) fired boiler," *JSME International Journal*, **41**, 1055 (1998).

Lefèbre, H., *Atomization and sprays*, Hemisphere Publishing Corporation, New York (1989).

Linak, W. P., Miller, C. A., Santoianni, D. A., Kink, C. J., Shinagawa, T., Wendt, J. O. L., Yoo, J. I. and Seo, Y. C., "formation of fine particles from residual oil combustion: Reducing nuclei through the addition of Inorganic sorbent," *Korean J. Chem. Eng.*, **20**, 664 (2003).

Ma, J., Fletcher, T. H. and Webb, B. W., "Conversion of coal tar to soot during coal pyrolysis in a post-flame environment," *Twenty-Sixthh Symposium (International) on Combustion*, The Combustion Institute, Pittsburgh, 3161 (1996).

Marrone, N. J., Kennedy, I. M. and Dryer, F. L., "Cokes formation in the combustion of isolated heavy oil droplets," *Combustion Science and Technology*, **36**, 149 (1984).

Miller, J. A. and Bowman, C. T., "Mechanism and modelling of nitrogen chemistry in combustion," *Progress in Energy and Combustion Science*, **15**, 287 (1989).

Nenniger, R. D., Howard, J. B. and Sarofim, A. F., "Sooting potential of coals," *International Conference on Coal Science*, Pittsburgh, 521 (1983).

Moleo, L. J., *Pollutant formation and interaction in the combustion of heavy liquid fuels*, PhD thesis, University college London (1998).

Northrop, P. S. and Gavalas, G. R., "Combustion characteristics of carbonaceous residues from heavy oil fired boilers," *Energy & Fuels*, **5**, 587 (1991).

Moszkowicz, P., Witzel, L. and Claus, G, "Modelling of very fast pyrolysis of heavy fuel oil droplets," *Chemical Engineering Science*, **51**, 4075 (1996).

Park, H. Y. and Kim, T. H., "Non-isothermal pyrolysis of vacuum residue (VR) in thermogravimetric analyzer," *Energy Conversion and Management*, **47**, 2118 (2006).

Park, H. Y. and Seo, S. I., "Numerical studies on the reaction of carbon particles in a vacuum residue air flame," *International Journal of Energy Research*, **30**, 365 (2006).

Pfefferle, L. D. and Churchill, S. W., "NO_x production from the combustion of ethane doped with ammonia in a thermally stabilized plug flow burner," *Combustion Science and Technology*, **48**, 235 (1986).

Richter, H. and Howard, J. B., "Formation of polyaromatic hydrocarbons and their growth to soot-a review of chemical reaction pathways," *Progress in Energy and Combustion Science*, **26**, 565 (2000).

Seeker, W. R., Samuelsen, G. S., Heap, M. P. and Trolinger, J. D., "Thermal decomposition of pulverised coal particles," *Eighteenth Symposium (International) on Combustion*, The Combustion Institute, Pittsburgh, 1213 (1980).

Serio, M. A., Hamblen, D. G, Markham, J. R. and Solomon, P. P., "Kinetics of volatile productevolution in coal pyrolysis: Experiment and theory," *Energy and Fuel*, **1**, 138 (1987).

Simbeck, D. and Johnson, H., "World gasification survey: Industry trends & developments," *Gasification Technologies 2001 Conference*, San Francisco, CA (2001).

Singer, J. G, *Combustion fossil power*, Combustion Engineering, Inc. Rand McNally (1991).

Sonoda, T., Komori, T., Kato, M., Kitauchi, Y., Iwasaki, Y., Akizuki, W., Hashi, T. and Kunihiro, K., "Development of M701F gas turbine for integrated gasification combined cycle plants," Technical Review, **41**, Mitsubishi Heavy Industries. Ltd. (2004).

Timothy, L. D., Froelich, D., Sarofim, A. F. and Beer, J. M., "Soot formation and burnout during the combustion of dispersed pulverised coal particles," *Twenty-First Symposium (International) on Combustion*, The Combustion Institute, Pittsburgh, 1141 (1986).

Urban, D. L., Huey, S. P. C. and Dryer, F. L., "Evaluation of the coke formation potential of residual fuel oils," *Twenty-Fourth Symposium (International) on Combustion*, The Combustion Institute, Pittsburgh, 1357 (1992).

Villasenor, R. and Escalera, R., "A highly radiative combustion chamber for heavy oil combustion," *International Journal of Heat and Mass Transfer*, **41**, 3087 (1998).

Villasenor, R. and Garcia, F., "An experimental study of the effects of asphaltenes on the heavy fuel oil droplet combustion," *Fuel*, **78**, 933 (1999).

Wolff, J., Radtke, K., Karg, J. and Gunster, W., "Refinery residue based IGCC power plants and market potential," *Gasification Technologies 2001 Conference*, San Francisco, CA (2001).